Dual-energy computed tomography for the differentiation of uric acid stones: ex vivo performance evaluation

Stolzmann, P ; Scheffel, H ; Rentsch, K ; Schertler, T ; Frauenfelder, T ; Leschka, S ; Sulser, T ; Marincek, B ; Alkadhi, H

Abstract: We assessed the potential of dual-energy computed tomography (CT) for the differentiation between uric acid (UA)-containing and non-UA-containing urinary stones. Forty urinary stones of 16 different compositions in two sizes (<and>or=5 mm) were examined in an ex vivo model. Thirty stones consisted of pure calcium oxalate (whewellite or wheddellite), calcium phosphate (apatite, brushite, or vaterite), ammonium magnesium phosphate (struvite), UA, ammonium acid urate, ammonium phosphate, sodium hydrogen urate, or cystine, and ten stones were of mixed composition (UA-sodium hydrogen urate, whewellite-urate, wheddellite-urate, whewellite-brushite, or whewellite-brushite-struvite). Scans were performed using dual-source CT in a dual-energy mode with the tubes simultaneously operating at 80 and 140 kV. Two readers analysed the data with respect to stone attenuation at each energy level. The stones were classified as UA- or non-UA-containing using manual attenuation measurements and software analysis results. Sensitivity, specificity, PPV, and NPV were calculated using crystallographic stone analysis as the gold standard. Twenty-six out of 40 stones (65%) contained no UA; 14 stones (35%) contained UA. When compared with UA-containing stones, the differences in attenuation values at 80 and 140 kV were significantly ($P < 0.001$) higher in stones containing no UA. The software automatically mapped 39/40 stones (98%). Only one (2%) 2 mm UA-stone was missed. The software correctly classified all detected stones as UA- or non-UA-containing. The attenuation values of the missed stone were manually plotted into the analysis sheet which allowed for the correct classification of the stone (containing UA). Therefore, the sensitivity, specificity, PPV, and NPV for the detection of UA-containing stones was 100%. Ex vivo experience indicates that differentiation between UA- and non-UA-containing stones can be accurately performed using dual-source dual-energy CT.

DOI: https://doi.org/10.1007/s00240-008-0140-x

Urol Res (2008) 36:133–138
DOI 10.1007/s00240-008-0140-x

ORIGINAL PAPER

Dual-energy computed tomography for the differentiation of uric acid stones: ex vivo performance evaluation

Paul Stolzmann · Hans Scheffel · Katharina Rentsch · Thomas Schertler · Thomas Frauenfelder · Sebastian Leschka · Tullio Sulser · Borut Marincek · Hatem Alkadhi

Received: 17 October 2007 / Accepted: 21 May 2008 / Published online: 11 June 2008

Abstract We assessed the potential of dual-energy computed tomography (CT) for the differentiation between uric acid (UA)-containing and non-UA-containing urinary stones. Forty urinary stones of 16 different compositions in two sizes (< and ≥ 5 mm) were examined in an ex vivo model. Thirty stones consisted of pure calcium oxalate (whewellite or wheddellite), calcium phosphate (apatite, brushite, or vaterite), ammonium magnesium phosphate (struvite), UA, ammonium acid urate, ammonium phosphate, sodium hydrogen urate, or cystine, and ten stones were of mixed composition (UA-sodium hydrogen urate, whewellite-urate, wheddellite-urate, whewellite-brushite, or whewellite-brushite-struvite). Scans were performed using dual-source CT in a dual-energy mode with the tubes simultaneously operating at 80 and 140 kV. Two readers analysed the data with respect to stone attenuation at each energy level. The stones were classified as UA- or non-UA-containing using manual attenuation measurements and software analysis results. Sensitivity, specificity, PPV, and NPV were calculated using crystallographic stone analysis as the gold standard. Twenty-six out of 40 stones (65%) contained no UA; 14 stones (35%) contained UA. When compared with UA-containing stones, the differences in attenuation values at 80 and 140 kV were significantly ($P < 0.001$) higher in stones containing no UA. The software automatically mapped 39/40 stones (98%). Only one (2%) 2 mm UA-stone was missed. The software correctly classified all detected stones as UA- or non-UA-containing. The attenuation values of the missed stone were manually plotted into the analysis sheet which allowed for the correct classification of the stone (containing UA). Therefore, the sensitivity, specificity, PPV, and NPV for the detection of UA-containing stones was 100%. Ex vivo experience indicates that differentiation between UA- and non-UA-containing stones can be accurately performed using dual-source dual-energy CT.

Keywords Dual energy · Computed tomography · Uric acid · Urinary stone

P. Stolzmann · H. Scheffel · K. Rentsch · T. Schertler · T. Frauenfelder · S. Leschka · T. Sulser · B. Marincek · H. Alkadhi (✉)
Institute of Diagnostic Radiology,
University Hospital Zurich, 8091 Zurich, Switzerland
e-mail: hatem.alkadhi@usz.ch

Introduction

Approximately 80% of all urinary stones are composed of calcium oxalate or calcium phosphate, 10% of struvite, 9% of uric acid (UA), and the remaining 1% of cystine or ammonium acid urate [1]. The ability to predict the stone composition before treatment enables the selection of patients who could potentially benefit from medical management rather than shock wave lithotripsy [2–4]. Even large UA stones are treated by urinary alkalization in combination with prior fragmentation by extracorporeal shock wave lithotripsy which is considered to be the reference management approach [1, 5, 6].

The method of choice for the diagnosis of urinary stone disease is non-contrast enhanced helical computed tomography (CT). It is recognised as the most accurate technique for detection of calculi in the urinary tract with a reported sensitivity of 95–100% [2, 7–9] The concomitant determination of the stones composition by CT would help the clinician in choosing the appropriate therapy. Early CT studies using a single energy technique have shown that the attenuation of stones in CT may provide some information

about their composition [2, 3]. However, a considerable overlap of attenuation values in single-source CT has been reported which precludes an accurate differentiation of stones with different chemical compositions [2, 3, 10, 11].

The most recently introduced dual-source CT scanner is composed of two X-ray tubes and two detectors that are orthogonally mounted onto the rotating gantry [12]. When running both tubes at the same tube voltage, a high temporal resolution is achieved which is primarily used for the evaluation of coronary arteries [13]. When operating both X-ray tubes at different tube voltages, the temporal resolution is lower. However, two different X-ray spectrums are simultaneously obtained and potentially improve tissue characterisation [12].

The purpose of this ex vivo study was to assess the value of dual-source CT simultaneously operated in the dual-energy mode for the differentiation between UA-containing and non-UA-containing urinary calculi using X-ray diffraction analysis as the gold standard.

Material and methods

Forty stones collected during surgical and endoscopic interventions were included in this study. A crystallographic analysis of the stones was performed prior to CT.

X-ray diffraction

The composition of the urinary stones was determined by X-ray diffraction. The urinary stone sample was pulverized and analysed by X-ray diffraction using a CubixPro diffractometer (PANalytical, Almelo, NL, USA) using Ni-filtered CuKα radiation. The crystalline components were identified using the ICDD database and the semiquantitative composition determined using the relative intensity of the different bands.

Urinary stone samples

The included 40 urinary stones consisted of 16 different compositions:

1. Thirty stones consisted of 11 pure compositions: calcium oxalate [i.e. whewellite and wheddellite (two times)], calcium phosphates (i.e. apatite (two times), brushite, and vaterite), ammonium magnesium phosphate (i.e. struvite), UA (two times), ammonium acid urate, ammonium phosphate, sodium hydrogen urate, or cystine (two times).
2. Ten stones consisted of five different mixed compositions: UA-sodium hydrogen urate (50%/50%), whewellite-urate (40%/60%), wheddellite-urate (20%/80%), whewellite-brushite-struvite (40%/30%/30%), or whewellite-brushite (80%/20%).

All of the stone compositions were available in two different sizes: 20 stones with a maximum transverse diameter smaller than 5 mm and 20 stones equal to or larger than 5 mm.

Work bench model

All stones were examined in an ex vivo work bench model placed on the dual-source CT scanner table. Stones were embedded in random order in fat ($20 \times 15 \times 8$ cm^3) representing the retroperitoneal, peri-renal, or para-ureteral fatty tissue, as previously shown [3] (Fig. 1a). This phantom was fully submerged under water in a tank ($35 \times 35 \times 25$ cm^3) in order to simulate normal human attenuation (Fig. 1b).

Data acquisition and reconstruction

The examinations of the model were performed on a dual-source CT scanner (Definition, Siemens Medical Solutions, Forchheim, Germany) in the dual-energy mode. The tube voltages were set at 80 and 140 kV, and the tube current time products at 400 and 95 mAs/rotation. The following scanning parameters were used: slice collimation $2 \times 32 \times 0.6$ mm, gantry rotation time 330 ms, and pitch 0.70. To test for reliability of the data, scans were performed two times.

The images from the 140 kV scan were reconstructed on the regular image reconstruction system of the CT scanner. Additional reconstructions from the raw spiral projection data of both tubes were performed on an external prototype workstation (Multi Modality Workplace, Prototype Soft-

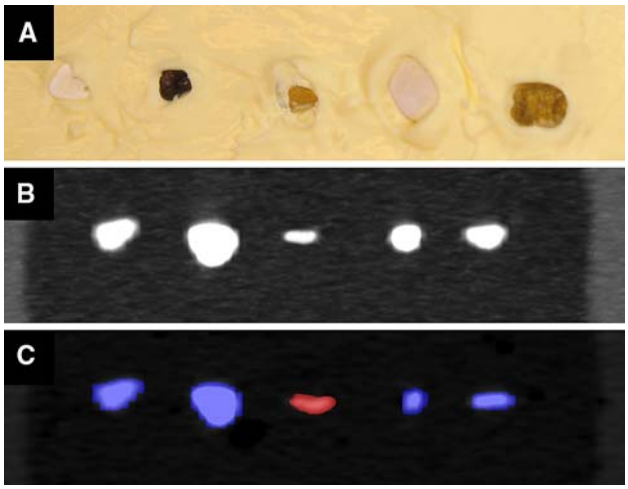

Fig. 1 Ex vivo urinary stone sample. **a** Collection of urinary stones embedded in butter during preparation. **b** CT image of stone sample in the work bench model. **c** CT image with colour-coded results obtained from the dual-energy CT data analysis. Uric acid-containing stones are labelled in *red*, non uric acid-containing stones are labelled *blue*

ware VA 13, Siemens). Transverse images were reconstructed with a slice thickness of 2 mm and an increment of 1.5 mm. The dual-energy data reconstruction was performed with a specifically designed soft tissue convolution kernel (D30f) in order to avoid changes of voxel information at objects' edges. Both readers used the fused images from both tubes (i.e. the 80 and 140 kV scans) for diagnostic purposes. MatLab algorithms were used to evaluate the 80 and 140 kV images with the intent to assign the content of voxels using three-material decomposition. The information of the voxel data was then transcribed into separate stacks of DICOM image files.

Data evaluation

Data sets were reviewed by a third-year resident and a board-certified radiologist with 8 years experience in reading abdominal CT. Each reader was blinded to the results from the other reader and was unaware of the chemical composition of the stones. The scans were presented only once in each reading session. Each reader was instructed to document the attenuation [in Hounsfield Units (HU)] of each stone in each series with standard metric software devices provided by the workstation. Measurements were performed by placing a region-of-interest (ROI) with a mean area of $3.7 \pm 1.4\ mm^2$ (range 1–7 mm^2). Then, the readers were asked to determine the presence or absence of UA using the dedicated kidney stones application of the dual-energy analysis software provided by the manufacturer (Siemens Medical Solutions, Forchheim, Germany). This software automatically calculates differences of attenuation between the 80 and 140 kV data sets and displays the results in a colour-coded fashion on fused multi-planar reformations (Fig. 1c).

During the first read-out, both readers independently performed the evaluation to test for inter-reader agreement. In order to evaluate the intra-reader agreement of attenuation measurements, one reader re-analysed the data sets after a 1-week period (second read-out). Inter-scan agreement was tested by one reader who additionally obtained attenuation measurements of the second scan. The reading order was randomized.

Statistical analysis

The results were expressed as absolute numbers, frequencies, and means ± SDs. The non-parametric Wilcoxon Signed Rank Test was performed to evaluate significant differences between the 80 and 140-kV series attenuation measurements, between scans, and between readers. Differences in attenuation at 80 and 140 kV were assessed using the Mann–Whitney *U* test between UA-containing and non-UA-containing urinary stones. A *P* level of <0.05 was considered statistically significant. The sensitivity, specificity, positive predictive value, and negative predictive value were calculated from Chi-Square tests of contingency. The 95% confidence intervals (CI) were calculated from binomial expression. All statistical analysis was conducted using SPSS software (12.0, Chicago, Ill, USA).

Results

The mean size of all 40 urinary stones was 4.5 ± 1.8 mm ranging from 2.0 to 7.0 mm. In the group of 20 stones smaller than 5 mm, the mean size was 2.9 ± 0.6 mm, ranging from 2.0 to 4.0 mm. The mean size in the group of the 20 stones equal to or larger than 5 mm mean size was 6.2 ± 0.8 mm, ranging from 5.0 to 7.0 mm.

A total of 14/40 stones contained UA (35%); 26 of 40 (65%) stones did not contain UA.

Intra-, inter-reader, and inter-scan agreement of attenuation measurements

No significant differences in attenuation value measurements were found between the first and second read-out when measurement obtained at 80 kV ($P_{80\,kV} = 0.98$) and at 140 kV ($P_{140\,kV} = 0.49$) were compared separately. Mean of both measurements was taken for subsequent analysis.

No significant differences in attenuation values were found for both readers at 80 kV ($P_{80\,kV} = 0.20$) and 140 kV ($P_{140\,kV} = 0.73$). The mean of both measurements were taken for subsequent analysis. Mean of all measurements was taken for subsequent analysis (Table 1).

We found no significant differences in attenuation values between both scans at 80 kV ($P_{80\,kV} = 0.27$) and 140 kV ($P_{140\,kV} = 0.70$).

Attenuation values at different tube voltages

At 80 kV, the mean attenuation was 775 ± 554 HU (range 64–1953). At 140 kV, the mean attenuation was 565 ± 328 HU (range 70–1,292) (Table 1). Attenuation values were significantly higher at 80 kV when compared with 140-kV scans ($P < 0.001$). Regarding the differences in attenuation (i.e. $\Delta HU = HU_{80\,kV} - HU_{140\,kV}$), mean differences in attenuation were 332 ± 289 HU for the non-UA-containing urinary stones and −20 ± 14 HU for the UA-containing stones. Differences in attenuation values significantly differed ($P < 0.001$) between both groups of urinary stones.

Diagnostic performance of the analysis software for detecting UA-containing stones

The dual-energy analysis software automatically mapped 39 out of 40 (98%) stones. Only one stone (UA, size 2 mm)

Table 1 Mean CT attenuation values at 80 and 140 kV of pure and mixed urinary stones

	Component	Number	Sizes (mm)	Attenuation at 80 kV (HU)	Attenuation at 140 kV (HU)
Pure stones	Whewellite	2	4/6	1,549	908
	Wheddellite	4	2/3/5/7	1,726	920
	Apatite	4	3/4/6/7	795	566
	Brushite	2	4/7	1,435	1,083
	Vaterite	2	2/5	807	429
	Struvite	2	3/6	603	516
	Uric acid	4	3/4/6/7	154	174
	Ammonium acid urate	2	3/6	285	301
	Ammonium phosphate	2	3/5	583	427
	Sodium hydrogen urate	2	2/5	152	162
	Cystine	4	2/3/6/7	604	460
Mixed stones	Uric acid-sodium hydrogen urate (50%/50%)	2	3/5	157	191
	Whewellite-urate (40%/60%)	2	3/7	566	583
	Wheddellite-urate (20%/80%)	2	2/6	244	262
	Whewellite-brushite-struvite (40%/30%/30%)	2	3/7	1,213	918
	Whewellite-brushite (80%/20%)	2	3/7	1,413	1,162

was missed. Thirteen out of 39 stones (33%) were classified by the software as containing UA, and therefore were highlighted with a reddish colour (Figs. 1c, 2). The results of the automated analysis of all 39 stones were in agreement with the crystallographic analysis. No false-positive and no false-negative ratings occurred using the software.

Thus, the sensitivity of dual-energy CT for the classification of urinary stones as containing UA was 100% (95% CI: 75–100%), the specificity was 100% (95% CI: 87–100%), the positive predictive value was 100% (95% CI: 75–100%), and the negative predictive value was 100% (95% CI: 87–100%).

Taking the unmapped stone as a false-negative rating into account, the sensitivity and negative predictive value of dual-energy CT for the classification of urinary stones as containing UA using the software were reduced to 93% (95% CI: 66–100%) and 96% (95% CI: 81–100%). The specificity and positive predictive value on the other hand remained constant at 100% (95% CI: 87–100%) and 100% (95% CI: 75–100%).

The attenuation values of the missed stone (as determined by ROI measurements) were 70 HU at 140 kV and 64 HU at 80 kV. When these measurements were manually plotted into the analysis sheet values, the stone could be correctly classified as containing UA (Fig. 2).

Discussion

Urinary stone disease is a common and increasing problem in daily urological practice. Shock wave lithotripsy is considered to be the reference treatment for most kinds of calculi [11]. On the other hand, shock wave lithotripsy may not be the technique of choice, nor a cost-effective option when alternative medical treatment options are suitable and potentially harmful shock waves for the renal parenchyma can be avoided [4]. Regarding UA-containing urinary stones, medical dissolution by urinary alkalization demonstrates the reference management technique before other treatment options are considered [1, 4–6]. These different therapy approaches are the driving force behind the efforts to determine the UA-component of urinary stones prior to treatment [11]. Concerning non-UA-containing stones, the differentiation seems to be of a lower value because the knowledge of the major stone component does not allow for the adequate prediction of its fragility in lithotripsy treatment [4].

In this study, we could demonstrate that UA-containing stones and non-UA containing stones can be accurately differentiated in an ex vivo setting using a dual-energy CT approach with the most recent dual-source CT scanner.

The dual-energy analysis technique provides valuable information related to the varying response of certain tissues to X-rays of different energies. Differences in the attenuation are based on the material-dependent Compton and photo-electric effects as described by Avrin and co-workers [14]. Thus, material differentiation and the prediction of urinary stone composition becomes possible with the application of different X-ray spectrums [2, 3, 15].

In some studies, even single-energy CT attenuation measurements of UA-containing stones significantly differed from other urinary stone compositions [2, 3]. On the other

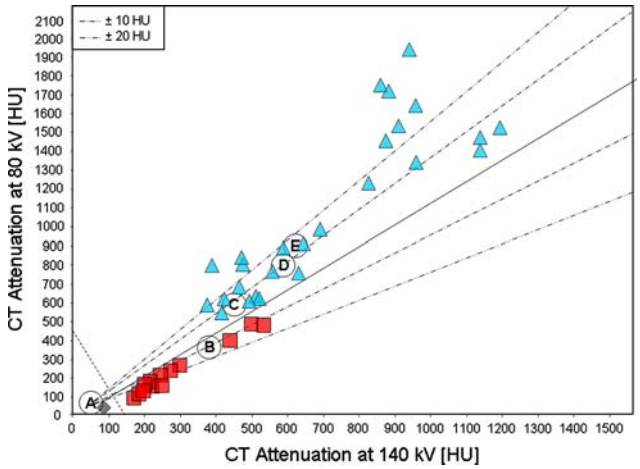

Fig. 2 The analysis sheet demonstrating substance-specific attenuation values at different tube voltages. The *solid reference line* plots the very similar dual-energy behaviour of normal tissue. Its ratio is set so that the overlay image is zero for average concentrations of heavy ions. The *dotted lines* represent positive and negative deviations from the solid reference line (*dot-dash* difference of ±10 HU from reference, *dot-dot-dash* ±20 HU from reference line). Negative deviations from the reference line are coded in *red* representing UA-containing stones (*red triangles*). Positive deviations are coded in blue representing non-UA-containing stones (*blue triangles*). The *left dashed line* demonstrates the lowest threshold for analysis. Below 100 HU, calculations are not performed by the software analysis tool anymore. One stone with attenuation values below the threshold was not automatically detected by the software, but was rated as UA-containing according to the manual measurements (*grey diamond*). The *capital letters* represent reference values provided by the manufacturer: **a** urine; **b** uric acid; **c** cystine; **d** apatite; **e** oxalate

hand, Motley and colleagues [10] reported that an accurate identification of different stones was precluded by a considerable overlap of attenuation values. In addition, a high variability of attenuation values that is caused by different detector collimations and stone sizes leading to volume inaccuracies has been described [16]. In order to avoid overlapping attenuation values, some authors have used an air-filled phantom [2], or only pure urinary stones [3]. In our study, we used the combination of 80 and 140 kV, which provided more consistent results caused by higher differences in attenuation [14]. The differences in attenuation obtained from the UA-containing stones significantly differed from those of non-UA containing stones when different X-ray spectrums were applied.

The dual-energy CT analysis software tool used in this study decomposes each voxel, and the software results are displayed in a colour-coded fashion on fused images of the 80 and 140-kV series. The colour depends on the voxel's distance from the reference of the average concentrations of heavy ions. In our study, this algorithm promised excellent results for all mapped stones. One stone was not detected by the software because it fell under the lowest threshold for calculations. Because the attenuation levels of the missed UA-containing stone were between 64 and 70 HU, assignments of the stones components were not performed. Since urinary stones with a low density may be overlooked by the analysis, measuring of attenuation values and using of the analysis sheet for a correct assignment are recommended.

However, the dual-energy material decomposition algorithm used by the software could be superior to manual attenuation measurements for the detection of small amounts of UA. The software decomposition includes both the periphery and inside voxels. Volume artefacts, therefore, do not adulterate results and even small UA components are detected [17]. With regard to the clinical situation though, it needs to be stated that only urinary stones that have UA as their major component can be treated medically.

With former single-source CT scanners, dual-energy data had to be separately acquired in two subsequent scans [2, 3, 15]. However, if minimal changes in the patient position, occur or if the breath is not held properly by the patient, the voxel decomposition will be false because both datasets do not contain the same structures anymore [18]. The dual-source CT scanner resolves this major drawback by the simultaneous acquisition of data [12, 15]. Another problem of former single-source CT scanners is that the tube current at lower tube voltages is not sufficient to gain images of diagnostic noise and resolution [19]. In our study, even with the use of a full water tank, the quality of low-voltage data was sufficient for the analysis of every stone.

Conclusion

The first ex vivo experience reported in this study indicates that dual-source dual-energy CT allows for the accurate differentiation between UA-containing and non-UA-containing stones. Further prospective studies are warranted in order to prove the feasibility of the chemical decomposition in an in-vivo setting and to assess the clinical value of the new technology.

Acknowledgments This research was supported by the National Center of Competence in Research, Computer Aided and Image Guided Medical Interventions of the Swiss National Science Foundation.

References

1. Coe FL, Evan A, Worcester E (2005) Kidney stone disease. J Clin Invest 115:2598–2608
2. Deveci S, Coskun M, Tekin MI, Peskircioglu L, Tarhan NC, Ozkardes H (2004) Spiral computed tomography: role in determination of chemical compositions of pure and mixed urinary stones—an in vitro study. Urology 64:237–240

3. Mostafavi MR, Ernst RD, Saltzman B (1998) Accurate determination of chemical composition of urinary calculi by spiral computerized tomography. J Urol 159:673–675
4. Williams JC Jr, Saw KC, Paterson RF, Hatt EK, McAteer JA, Lingeman JE (2003) Variability of renal stone fragility in shock wave lithotripsy. Urology 61:1092–1096 (discussion 1097)
5. Ngo TC, Assimos DG (2007) Uric Acid nephrolithiasis: recent progress and future directions. Rev Urol 9:17–27
6. Liebman SE, Taylor JG, Bushinsky DA (2007) Uric acid nephrolithiasis. Curr Rheumatol Rep 9:251–257
7. Boulay I, Holtz P, Foley WD, White B, Begun FP (1999) Ureteral calculi: diagnostic efficacy of helical CT and implications for treatment of patients. AJR Am J Roentgenol 172:1485–1490
8. Dalrymple NC, Verga M, Anderson KR, Bove P, Covey AM, Rosenfield AT, Smith RC (1998) The value of unenhanced helical computerized tomography in the management of acute flank pain. J Urol 159:735–740
9. Yilmaz S, Sindel T, Arslan G, Ozkaynak C, Karaali K, Kabaalioglu A, Luleci E (1998) Renal colic: comparison of spiral CT, US and IVU in the detection of ureteral calculi. Eur Radiol 8:212–217
10. Motley G, Dalrymple N, Keesling C, Fischer J, Harmon W (2001) Hounsfield unit density in the determination of urinary stone composition. Urology 58:170–173
11. Sheir KZ, Mansour O, Madbouly K, Elsobky E, Abdel-Khalek M (2005) Determination of the chemical composition of urinary calculi by noncontrast spiral computerized tomography. Urol Res 33:99–104
12. Flohr TG, McCollough CH, Bruder H, Petersilka M, Gruber K, Suss C, Grasruck M, Stierstorfer K, Krauss B, Raupach R et al (2006) First performance evaluation of a dual-source CT (DSCT) system. Eur Radiol 16:256–268
13. Scheffel H, Alkadhi H, Plass A, Vachenauer R, Desbiolles L, Gaemperli O, Schepis T, Frauenfelder T, Schertler T, Husmann L et al (2006) Accuracy of dual-source CT coronary angiography: first experience in a high pre-test probability population without heart rate control. Eur Radiol 16:2739–2747
14. Avrin DE, Macovski A, Zatz LE (1978) Clinical application of Compton and photo-electric reconstruction in computed tomography: preliminary results. Invest Radiol 13:217–222
15. Johnson TR, Krauss B, Sedlmair M, Grasruck M, Bruder H, Morhard D, Fink C, Weckbach S, Lenhard M, Schmidt B et al (2007) Material differentiation by dual energy CT: initial experience. Eur Radiol 17:1510–1517
16. Saw KC, McAteer JA, Monga AG, Chua GT, Lingeman JE, Williams JC Jr (2000) Helical CT of urinary calculi: effect of stone composition, stone size, and scan collimation. AJR Am J Roentgenol 175:329–332
17. Primak AN, Fletcher JG, Vrtiska TJ, Dzyubak OP, Lieske JC, Jackson ME, Williams JC Jr, McCollough CH (2007) Noninvasive differentiation of uric acid versus non-uric acid kidney stones using dual-energy CT. Acad Radiol 14:441–447
18. Grosjean R, Sauer B, Guerra RM, Daudon M, Blum A, Felblinger J, Hubert J (2008) Characterization of human renal stones with MDCT: advantage of dual energy and limitations due to respiratory motion. AJR Am J Roentgenol 190:720–728
19. Kelcz F, Joseph PM, Hilal SK (1979) Noise considerations in dual energy CT scanning. Med Phys 6:418–425